Integrative Biology

Accepted Manuscript

ROYAL SOCIETY OF CHEMISTRY

www.rsc.org/ibiology

Inhibition of Cell-Cell Adhesion Impairs Directional Epithelial Migration on Micropatterned Surfaces

Kathryn E. Worley[1], David Shieh[2], Leo Q. Wan[1,3,4*]

1 Department of Biomedical Engineering

2 Department of Biology

3 Center for Biotechnology & Interdisciplinary Studies

4 Center for Modeling, Simulation and Imaging in Medicine

*Correspondence to:

Assistant Professor of Biomedical Engineering

Laboratory for Tissue Engineering and Morphogenesis

2147 Center for Biotechnology & Interdisciplinary Studies

Rensselaer Polytechnic Institute

110 8th Street, Troy NY 12180

518-276-2505 (Office)

518-276-3035 (Fax)

wanq@rpi.edu

http://www.rpi.edu/~wanq

Keywords: Cell Chirality, Cell Adhesion, Collective Cell Migration, Micropatterning, Left-Right Asymmetry, Tissue Morphogenesis

Abstract

The development of the vertebrate body plan with left-right (LR) asymmetry (also known as handedness and chirality) requires the emerging chiral morphogenesis of epithelial cells at specific embryonic stages. In this process, cell-cell adhesions coordinate cellular organization and collective cell migration, and are critical for the directional looping of developing embryonic organs. However, the underlying biophysical mechanism is not yet well understood. Here we modeled normal and delayed epithelial LR symmetry breaking with patterned epithelial chiral morphogenesis on microscale lines with various widths. The patterned cells exhibited biased migration wherein those on opposing boundaries migrated in different directions. Disrupting adherens junctions with ethylene glycol tetraacetic acid (EGTA) resulted in a decrease in velocity difference in opposing boundaries as well as the associated biased cell alignment, along with an increase in the overall random motion. Altering the distance between the opposing boundaries did not significantly alter alignment, but significantly disturbed the velocity profile of the cell migration field. Further examination of cell polarity indicated that disruption of adherens junctions did not affect cell polarization on the boundaries, but decreased the transmission of chiral bias into the interior region of the epithelial cell sheet. Overall, our results demonstrated the dependence of the scale of collective cell migration on the strength of cell-cell adhesion, and its effects on the chirality of a multicellular structure through mediating cell polarity in the vicinity of geometric boundaries. This study demonstrated that our 2D microscale system provides a simple yet effective tool for studying the influence of collective cell migration on LR symmetry breaking, and possibly for fetal drug screening to prevent birth defects related to alteration in cell-cell adhesion.

Introduction

Tissue morphogenesis is a complex process involving drastic epithelial cell migration, which leads to collective cell behaviors such as convergence, extension, invagination, rotation and looping, and culminates in the formation of a functional organism with properly placed tissues, organs and organ systems. Left-right (LR) asymmetry, or chirality, is widely observed during tissue morphogenesis, and considered as a well-conserved characteristic in living organisms at all hierarchical levels,[1-4] including the twisting of snail shells and positioning of human internal organs. The disruption of normal LR asymmetry leads to birth defects in laterality, often as a result of heritable genetic diseases such as Kartagener syndrome or prenatal exposure to teratogens.[5] Recent studies indicate that many LR symmetry-breaking events such as heart and gut looping are due to intrinsic chirality within the tissue,[6,7] through vast organization and reorganization, and directional migration of cells within a multicellular planar structure. In particular, cell-cell adhesion plays a significant role in this collective chiral process. For instance, it was reported that blocking the expression of the cell-cell adhesion molecule, N-cadherin, at HH stage 3-4 randomized heart looping of chicken embryos.[8] Therefore, studying the role of similar epithelial cell-cell adhesion molecules and their influence on collective migration is of interest for exploring LR asymmetry in development and disease.

Previously, we have demonstrated cell chirality at a multicellular level for the first time using an *in vitro* model.[9-12] When cells were constrained between two micropatterned appositional boundaries (such as in rings and long strips), the cell monolayer in-between exhibits a biased alignment, the chirality of which depends on cell phenotype and cytoskeletal function.[9] Subsequently, such a chiral phenomenon has been reported in other similar systems.[13,14] For instance, vascular mesenchymal cells formed chiral patterns on surfaces containing alternating

fibronectin lanes and cell non-adhesive polyethylene glycol (PEG) lanes, and such patterns expanded into the entire surface with PEG degradation.[14] Recapitulating chiral morphogenesis using *in vitro* models provides us with an opportunity to interrogate the biophysical mechanisms of how multicellular chirality is established.

Single cells were demonstrated to be chiral,[15] but it is not clear how single cell chirality can be transformed into a multicellular level. We hypothesize that cell-cell adhesion plays a significant role through coordinating cell migration and cell polarity. To this end, we have studied Madin-Darby canine kidney (MDCK) cells, a widely used epithelial cell line, cultured on 2D long strip patterns with a varying width under the treatment of ethylene glycol tetraacetic acid (EGTA), a calcium chelator capable of disrupting cadherin junctions. We find a distinct profile of directional epithelial migration, associated with the biased cell alignment observed on line patterns, and this migrational bias decreases with weakening in cell-cell adhesion and a reduced size of underlying geometry (ie, line width). We infer that the development of specific cell-cell interactions at a specific stage when the organ has a proper size may be important for LR asymmetry in embryonic development. This study demonstrates that our 2D microscale system provides a simple yet effective tool for studying tissue morphogenesis, and possibly for fetal drug screening to prevent birth defects related to disruption of collective migration.

Material and Methods:

Cell Culture

Madin-Darby canine kidney epithelial cells (MDCK) (ATCC® CCL-34™) were maintained with complete Dulbecco's Modified Eagle Medium (Life Technologies) with 10% fetal bovine serum (Sigma) in tissue culture flasks. Once reaching 100 % confluency the cells were trypsinized and seeded onto the fibronectin-coated micropatterned surfaces.

Microcontact Printing

The microcontact patterning is performed using a gold-coated glass slide method.[9] A chromium mask was used to transfer geometric features (ie, line patterns of various widths) to a silicon wafer master mold using SU-8 2050 photoresist (Micro-Chem). Polydimethylsiloxane (PDMS; Corning) stamps were created using this master mold. The stamps were then used to transfer the adhesive self-assembly monolayer (SAM), octadecanethiol (Sigma), to gold-coated slides. The background was subsequently blocked through immersion of the slides in a non-adhesive ethylene glycol-terminated SAM ((HS-$(CH_2)_{11}$-EG_3, Prochimia). The patterned gold-coated slide was then washed with ethanol, dried, and treated with 10 μg/mL of fibronectin (Sigma) before cell seeding.

Cell Patterning

The cells were allowed to attach until the patterns were at approximately 50 % confluency, and any excess cells were washed off with fresh media. Ethylene glycol tetraacetic acid (EGTA) (Sigma), a calcium chelating agent, was then added to the media to remove calcium ions, thereby disrupting the calcium-dependent cadherin bonds. Cells were treated with either 0, 0.5 mM or 1 mM EGTA and their migration on line array patterns observed.

Time Lapse imaging

Time lapse imaging was performed at 37 °C and 5% CO_2 in a Zeiss Axio Observer with XL incubator for 18 to 24 hours after cell seeding. Phase contrast images were taken at a rate of 5 minutes per frame. For single cell imaging, the cells were sparsely seeded and images were taken every 5 minutes for approximately 3 hours.

Analysis of Cell Migration

The time lapse videos of confluent lines were analyzed using MATLAB. For easier processing, the videos were first cropped and rotated using ImageJ so that the micropatterned line was aligned in the vertical direction. Cell migration was analyzed using the MatPIV program.[9] In this program, Fast Fourier transform (FFT) was utilized to match regions of two sequential phase contrast images to estimate local displacements of sub-regions. The overall average speed was defined as the mean of speed, average change in local displacements divided by the time interval, over an entire line segment for all time points. The velocity difference between the left and right boundaries was determined by subtracting the vertical velocity of the left boundary from that of the right.

Single cell migration was tracked manually using an ImageJ plugin, MTrackJ.[9] Individual cells were tracked frame by frame, and the overall average speed of a cell was determined as the total travel distance divided by the time.

Analysis of Chiral Cell Alignment

Cell alignment was determined by running the same videos used for the cell migration analysis through a custom-written MATLAB program.[9] The program is based on the automated detection of intensity gradient of phase contrast images of the cells.[16] The biased angle was determined by examining the cell alignment in relation to the left boundary of the line pattern. The angle is between -90°and +90° with 0° being perpendicular to the boundary. The reported angle of alignment was the average across the entire line.

Immunofluorescence Staining

Cells were fixed using 4% paraformaldehyde or a cytoskeletal buffer fixative and blocked for 30 minutes at 37 °C using bovine serum albumin (5% in 1X Tris buffered saline, Sigma). The presence of E-cadherin was determined by incubating the cells with anti-E-cadherin-FITC

antibody (5 μg/mL, BD Bioscience) for 1 hour. The centrosome was visualized through the use of monoclonal anti-α-tubulin FITC (1:30 dilution, Sigma). All slides were mounted using a mounting medium containing, 4',6-diamidino-2-phenylindole, DAPI (Vectashield).

Statistical Analysis

The statistical analysis was performed using the statistical computing software R.[17] One or two way analysis of variance (ANOVA) was used with the Tukey's honest significance (HSD) post-hoc test. One-way ANOVA was performed for the 200 μm line widths to determine the influence of EGTA concentration on alignment, the velocity difference between the left and right boundaries, overall speed and single cell speed. One sample t-tests were also performed for the differences at the boundaries to ascertain whether the difference was statistically different from zero ($\mu_0 = 0$). Two-way ANOVA was performed to determine the influence of width and EGTA concentration on the variations in alignment, the velocity difference between the left and right boundaries, and overall speed. Tukey's HSD post-hoc tests were performed at a 95% confidence level to assess significance. The p values were reported for post-hoc tests, unless noted otherwise. Data appear as mean ± standard deviation. Error bars in all graphs are displayed as standard error.

Results

Disruption of Adherens Junctions Diminishes Epithelial Cell Chiral Alignment

Madin-Darby canine kidney (MDCK) epithelial cells on 200 μm line patterns displayed a chiral alignment (Figure 1a), as observed for other cell types previously reported.[9] If a cell is followed downwards, it tends to point toward the left side (Figure 1a). To determine the role of adherens junctions in the establishment of chirally aligned epithelial cells, the cells were treated with EGTA at 0, 0.5, and 1 mM (Figure 1 a-c). EGTA is a calcium chelating agent, and is commonly

used to disrupt the calcium-dependent cadherin/cadherin bonds of adherens junctions.[18] In untreated MDCK cells (Figure 1d) E-cadherin was found to primarily localize at cell-cell boundaries. In contrast, E-cadherin was more localized in the interior of the cell (Figure 1e-f), with little observed at the cell-cell boundaries for 1 mM EGTA treatment (Figure 1f), indicating an effective disruption of adherens junctions. We quantified cell alignment by determining the intensity gradient of phase contrast images of lines (Figure S1).[9] The average angle of alignment (relative to the left boundary) was found to decrease with EGTA concentration with a statistically significant decrease between the control and the 1 mM EGTA treatment group ($p = 0.014$; Figure 1g).

Migrational Bias Decreases with Disruption of Cell-Cell Adhesion, while Cell Motility Increases.

The formation of cell chiral alignment on micropatterns coincides with asymmetrical cell migration on opposite boundaries. For untreated cells, cells on the left boundary moved downwards, while those on the right upwards. Such directional migration on boundaries was able to maintain even after cells were overconfluent for many hours. The difference in velocity between the two boundaries (-0.54 ± 0.18 μm/min) was significantly different from zero ($p = 0.00022$; Figure 2a), and therefore cell migration on boundaries was chiral. When compared to the EGTA treated groups, this velocity difference was significantly larger ($p = 0.036$, ANOVA). We suspected that diminishing chiral alignment was due to a decrease of cell motility. An examination of the average speed of the cell monolayer showed a slight increase with EGTA treatment (Figure 2b), from 0.39 ± 0.04 μm/min for control to 0.60 ± 0.26 μm/min for 1 mM EGTA. However, the results were not statistically significant within our specified confidence level of 95% ($p = 0.062$, ANOVA). An analysis of single cell motility did show a statistically

significant increase, from 0.45 ± 0.34 μm/min for the control to 0.84 ± 0.34 μm/min for 1 mM EGTA ($p < 1.7E-05$; Figure 2c). These results indicate that while EGTA does influence the migration rate of individual MDCK cells, cell motility itself does not seem to be a driving force behind the establishment of chiral alignment.

Disruption of Cell-Cell Adhesion Disturbs the Distinct Linearly Varying Velocity Profile.

We further examined the velocity profiles across the width of line patterns under the EGTA treatment conditions (Movie S1-2), since the formation of chiral alignment requires cell migration in a coordinated fashion, ie, collective cell migration. The velocity profile across the width of a 200 μm control line shows plateau regions, regions where cells are migrating at a uniform speed near the two edges, connected by a single linearly varying region (Figure 3a), referred to in subsequent figures as 'One Linear Region'. These velocity profiles were created through an averaging of the parallel velocities across the width of the line for all time points. This profile illustrates that over time the migration for the control lines is incredibly consistent with cells on the left boundary migrating downward and those on the right migrating upward. The conflicting boundary information creates an area in the middle, the distinct linearly varying region, also referred to as the linear region, in which cells are receiving information from both boundaries. This conflicting information influences the interior cells' migration directionality creating an area near the center of the line wherein cells migrate very little or are constantly switching direction resulting in an average velocity of zero in the velocity profile. Line patterns treated with EGTA, however, show a more diverse velocity profile (Figure 3b-c), as quantified by the number of linear regions (Figure 3d). The presence of more than one linear region is denoted as 'Multiple Linear Regions' in all related figures. The more diverse velocity profile after EGTA treatment suggests that there is a less coherent transmission of migration information

throughout the cell sheet likely due to the decrease in cell-cell adhesion. The presence of the plateau regions at the two boundaries leads us to believe that there is a characteristic length (perpendicular to the boundary) where cells are collectively migrating at the same speed in the same direction. The characteristic length affects the formation and stability of chiral patterns.

Decreasing Line Width Affects Velocity Profile

To directly elucidate the role of this characteristic length, presumably influenced by the extent of cell-cell adhesion, on the scale of chiral alignment formation, we varied the width of patterned lines (Movie S3-4), and examined the plateau and linear regions of the velocity profiles as shown in Figure 3a. For the control, when the line width decreases from 200 μm to 100 μm, the velocity profile still maintained a distinct linearly varying region (Figure 4a). The 50 μm patterns, which are two to four cells across, have a large chance (~ 40%) of displaying a velocity profile that does not change across the width of the line (ie, no linear regions), which indicates that all cells in the line are migrating in the same direction, at a similar speed (Supplemental Figure 2).

The number of linear regions increased significantly with EGTA concentration and line width (Figure 4b-c). In particular, the percentage of a single linear region is highest at 100 μm for both EGTA groups. When the width decreased to 50 μm, a similar percentage of lines with no linear regions (ie, ~40%) were found as in the control group.

A detailed quantification of the velocity profile shows that the length of plateau region decreased on a narrower line ($p = 0.0091$, ANOVA) and with EGTA treatment ($p = 7.0E-04$, ANOVA; Figure 4d). For the control group, the characteristic length is 44 ± 32 μm on 200 μm-width lines, and 15 ± 1.6 μm on 50 μm-width lines ($p = 0.029$). In contrast, when treated with 1 mM EGTA, the length becomes 33 ± 19 μm for 200 μm lines, and 12 ± 4.6 μm for 50 μm lines. When normalized by the line width (Figure 4e), the plateau region showed a slight decrease in

percentage with increasing line width ($p = 0.056$, ANOVA), suggesting that the scale of plateau region is not simply proportional to line width. The relationship to EGTA concentration was statistically significant ($p = 0.013$, ANOVA) indicating that decreasing cell-cell adhesion is related to the decrease in collective migration along the boundaries. All data suggest that the scale of directional collective migration at boundaries decreases with a reduction in cell-cell adhesion, and can be affected by the underlying pattern size.

Effects of Pattern Size on Chiral Morphogenesis

After determining the influence line width has on the velocity profile, we examined how this width influences the ability of the cells to align and create a chiral bias on the line patterns. We did not find much change in chiral alignment between the 100 μm and 200 μm untreated lines, but there was a slight decrease in biased alignment for cells on the 50 μm line pattern (Figure 5a). The EGTA treatment decreased biased alignment, and this was observed for all line widths ($p = 9.7E-05$, ANOVA; Figure 5a).

The differences in velocity between the opposing boundaries showed similar trends with that of the alignment, but line width was also found to have a statistically significant effect ($p = 0.002$ Concentration; $p = 1.3E-04$ Width, two-way ANOVA). For the control, decreasing the line width significantly reduced the velocity difference between boundaries (200 μm v. 50 μm: $p = 0.003$). When EGTA concentration increased from 0 mM to 1 mM, a significant decrease in velocity difference was observed for 100 μm ($p = 0.015$) and 200 μm patterns ($p = 0.062$; Figure 5b). The overall average speed did not change much with the variation of line width, although a slight decrease of speed was perceived for the control (Figure 5c; 0.30 ± 0.03 for 50 μm lines vs 0.39 ± 0.04 for 200 μm lines). EGTA treatment was shown to be a more significant factor influencing overall speed ($p = 0.0019$, ANOVA). Higher concentrations of EGTA increased the overall

average speed, with statistically significant differences detected ($p = 0.0032$, ANOVA) between the 1 mM EGTA group and the control, while no significant difference was found between the control and the 0.5 mM EGTA group (Figure 5c).

Taken together, these data suggest the scale of multicellular structure can significantly affect the cell chiral alignment and biased migration, without a drastic influence on overall migration speed.

Coordinated Cell Polarity Mediates In Vitro Chiral Morphogenesis

Compared to the random collective migration of a cell cluster in an open space, the collective migration of the cells near the boundaries are directionally biased. We further looked into how the directional bias was transmitted into the interior region (in a distance of several cell width) of the patterned line. For this purpose, we examined the internal polarization by focusing on the location of the centrosome in relation to the nucleus. Cells on the boundary, regardless of treatment, exhibit a consistent localization of the centrosome between the boundary and the nucleus with the centrosome situated toward the leading edge of the cell (Figure 6a-c). As we progress through to a more interior region approximately 2-3 cell widths (~ 30 um) from the boundaries we see, for the control lines, an internal polarization similar to that seen for the cells directly contacting the corresponding boundary. This propagation of boundary information seems to be less prominent under EGTA treatment based on the more random internal polarization of these interior region cells (Figure 6b,c). Taken together, our data suggest that disruption of adherens junctions doesn't affect cell polarization at the boundary, but decreases the transmission of chiral bias in the epithelial cell sheet.

Discussion

Our objective was to investigate how cell-cell adhesion affects chiral morphogenesis of epithelial cells in a geometrically-defined multicellular structure. Using micropatterning techniques, we showed that disruption of adherens junctions diminished the capability of MDCK cells to establish chiral alignment on the patterned substrate, accompanied by a decrease in directional migration on the boundaries and a deviation from the distinct linearly-varying velocity profile of non-treated epithelial cells. In addition, varying geometrical size altered chiral alignment and directional migration of epithelial cells on patterned boundaries. Taken together, these data suggest that epithelial chiral morphogenesis can be regulated by varying cell-cell adhesion, and is influenced by the size of a multicellular structure.

In this study, we used dog kidney epithelial cells, or MDCK cells as a model for multiple reasons. First, MDCK is one of the most studied epithelial cells for various applications including collective cell migration, and their properties are well characterized. Second, while the kidneys are seemingly symmetric organs there is in fact a distinct asymmetry in size between the two kidneys with the left being larger than the right.[19-21] More importantly, there are also several genes that when disrupted cause alterations in both left-right asymmetry and kidney function,[22-24] indicating that similar pathways regulate both. Therefore, we chose the MDCK cells line as a suitable model for studying the influence of collective migration on chirality.

The chirality of multicellular morphogenesis (Figure 1) is initiated at the boundaries and propagated towards the interior regions through cell-cell contacts. At boundaries, the cells showed definite cellular polarization, and positioned their centrosome, rather than nuclei, closer to the boundary.[9,25] We observed that as cells polarized towards the boundaries of the line pattern on appositional boundaries, the cells biasedly migrated in opposite directions along the pattern itself. We quantified this bias through detection of a difference in velocity between the two

boundaries (Figure 2). Polarization at the border of an epithelial cell cluster is a common occurrence often times seen in the case of wound healing.[26] Due to the confined nature of the cells, they are unable to migrate outward into the open space causing them to migrate along the boundary of the micropattern. Such a difference on appositional boundaries eventually generates a shear flow-like field of cell migration, which results in the chiral alignment of both boundary and interior cells observed on the micropatterns. We would expect a similar outcome with other methods that are capable of generating comparable line features. Microcontact printing directly onto a petri-dish has previously been used to study chirality and no difference was seen between the gold-slide and petri-dish methods.[9] Creating lines using a channel method would create a physical barrier and assuming that the channel walls are non-adhesive, it is likely that the results would be similar because migration through a channel and on micropatterns is similar.[27,28]

The extent of chirality of patterned cells highly depends on cell-cell interactions. E-cadherin is known to link to the actin cytoskeleton,[29] although the exact mechanism is not yet fully understood.[30] Epithelial cell sheets have been previously shown to lose collective migration directionality under both EGTA treatment and E-cadherin antibody treatment.[31] The loss in collective migration in their system and ours is likely due to a reduction in the transmission of information between cells. The linking of cells' actin cytoskeletons at the sites of adherens junctions has been shown to facilitate force transmission in several different systems.[32] When cells are seeded sparsely, random walk is likely to dominate over any directional bias. We see that when more cells are in a confined region, cellular random movement is largely inhibited (Figure 2c vs 2b). Restricted movement has been shown to force cells to move together.[33] The presence of cell-cell adhesion further enhances collective cell migration. Thus, cells tend to migrate in clusters rather than individually.[34-37] Such kind of clustered migration can be

appreciated from the presence of plateau regions close to boundaries in the velocity profile (Figure 3a). The size of the cluster or plateau region increases with the strength of cell-cell adhesion. Using EGTA, we were able to decrease cell-cell adhesion while maintaining cell motility and found a decrease in the length of plateau regions. In addition, due to decreased cell-cell adhesion, the cells were less able to transmit boundary information to the interior region resulting in the disappearance of a single distinct linearly varying region connecting the plateau regions and replacement with multiple linear regions. The sum of these changes led to the observed loss of chirality due to the EGTA treatment. A visual representation (Figure 7) of these results illustrates the biased collective movement of untreated epithelial cells migrating along opposing boundaries and the effect of disrupting cell-cell adhesion on this collective behavior. The diagram displays several of the possible alterations in migration that occur after an effective disruption of cell-cell adhesion.

The scale of patterned geometry is another important consideration for chiral morphogenesis. When the line is broad, the biased alignment or migration on boundaries cannot be easily transferred to the interior region, which is far away (compared to cell size) from boundaries. When it is narrow, the clustered movement on two boundaries will affect each other, and effectively decrease the size of the cluster, ie, the length of plateau region, as observed in Figure 4d. In an extreme case (50 μm lines), cell movement on two boundaries was found to synchronize and move in the same direction (Figure 7). A study examining MDCK migration outward from a line showed independent migration at the boundaries for lines greater than 150 μm in width.[37] A similar line width of 100 μm was determined to be the best for strong chiral patterns to be observed for the control MDCK cells.

The chiral migration behavior of the cells leads to questions regarding the migration at the ends of the lines. The micropatterned line is a very long rectangle with the length being substantially longer than the width. We observed that with wider lines (e.g., 200 μm in width), the entire line can be divided into several segments, and in each segment there is generally a flow at the ends creating a cycling of cells. For example at the bottom end of a segment, cells on the left boundary migrate downward, to the right at the end boundary and then migrate upward on the right side. While this cyclic flow corresponds to wider lines, the flow of cells on the 50 μm line is unidirectional and therefore this type of flow is not observed. It is possible that non-uniformity in proliferation and/or build-up of cells due to migration creates areas of less and more cells. Over time, flow on 50 μm lines may shift direction, based on the cell density with cells migrating from areas of higher cell density to lower cell density. Once the cells become over confluent it is possible that migration will slow substantially as has been seen previously.[36] In addition, the cell density of an epithelial layer can be maintained by extruding cells from the monolayer when it is over-confluent.[38]

LR asymmetry breaking events are often associated with directional migration such as at Hensen's node in chick development,[39] and at the primary heart field during zebra fish heart development.[40] Our findings suggest that the success of epithelial related asymmetry breaking events will depend on properties such as; cadherin expression and the geometrical size of the organ/ tissue structure when it happens. Indeed, it was reported that blocking of N-cadherin expression at HH stage 3-4 randomized heart looping of chicken embryos.[8] It is therefore expected that insufficient or delayed expression in specific cell-cell adhesion molecules, such as E-cadherin, examined here, is likely to induce similar birth defects in laterality.

In summary, epithelial cell chiral alignment is accompanied by collective directional migration on micropatterned boundaries and is dependent on both cell-cell adhesion and the underlying geometrical shape. The scale of collective cell migration depends on the strength of cell-cell adhesion, and affects the chirality of a multicellular structure in a size-dependent manner. Our simple yet robust *in vitro* platform provided deep insights into collective cell migration in tissue chiral morphogenesis.

Acknowledgements:

The authors would like to thank National Science Foundation, American Heart Association, and March of Dimes for funding Support. Leo Q. Wan is a Pew Scholar in Biomedical Sciences, supported by the Pew Charitable Trusts.

Author Contributions:

K.E.W. and L.Q.W. designed research. K.E.W. carried out experiments, and conducted analysis. D.S. did some immunohistological staining and contributed to data interpretation. K.E.W. and L.Q.W. wrote the manuscript. L.Q.W. oversaw the project.

Competing Financial Interests:

The authors declare no competing financial interests.

References:

1 Tabin, C. J. The key to left-right asymmetry. *Cell* **127**, 27-32; (2006).

2 Levin, M. Left-right asymmetry in vertebrate embryogenesis. *Bioessays* **19**, 287-296; (1997).

3 Brown, N. A. & Wolpert, L. The development of handedness in left/right asymmetry. *Development* **109**, 1-9; (1990).

4 Speder, P., Petzoldt, A., Suzanne, M. & Noselli, S. Strategies to establish left/right asymmetry in vertebrates and invertebrates. *Curr Opin Genet Dev* **17**, 351-358; (2007).

5 Aylsworth, A. S. Clinical aspects of defects in the determination of laterality. *Am J Med Genet* **101**, 345-355; (2001).

6 Noel, E. S. *et al.* A Nodal-independent and tissue-intrinsic mechanism controls heart-looping chirality. *Nature communications* **4**, 2754; (2013).

7 Hatori, R. *et al.* Left-right asymmetry is formed in individual cells by intrinsic cell chirality. *Mechanisms of development*; (2014).

8 Garcia-Castro, M. I., Vielmetter, E. & Bronner-Fraser, M. N-Cadherin, a cell adhesion molecule involved in establishment of embryonic left-right asymmetry. *Science* **288**, 1047-1051; (2000).

9 Wan, L. Q. *et al.* From the Cover: Micropatterned mammalian cells exhibit phenotype-specific left-right asymmetry. *Proc Natl Acad Sci U S A* **108**, 12295-12300; (2011).

10 Wan, L. Q. & Vunjak-Novakovic, G. Micropatterning chiral morphogenesis. *Communicative & integrative biology* **4**, 745-748; (2011).

11 Singh, A. V. *et al.* Carbon nanotube-induced loss of multicellular chirality on micropatterned substrate is mediated by oxidative stress. *ACS Nano* **8**, 2196-2205; (2014).

12 Wan, L. Q., Ronaldson, K., Guirguis, M. & Vunjak-Novakovic, G. Micropatterning of cells reveals chiral morphogenesis. *Stem cell research & therapy* **4**, 24; (2013).

13 Deforet, M., Hakim, V., Yevick, H. G., Duclos, G. & Silberzan, P. Emergence of collective modes and tri-dimensional structures from epithelial confinement. *Nature communications* **5**, 3747; (2014).

14 Chen, T. H. *et al.* Left-Right Symmetry Breaking in Tissue Morphogenesis via Cytoskeletal Mechanics. *Circulation research*; (2012).

15 Xu, J. *et al.* Polarity reveals intrinsic cell chirality. *Proc Natl Acad Sci USA* **104**, 9296-9300; (2007).

16 Karlon, W. J. *et al.* Measurement of orientation and distribution of cellular alignment and cytoskeletal organization. *Ann Biomed Eng* **27**, 712-720; (1999).

17 R: A language and environment for statistical computing (R Foundation for Statistical Computing, Vienna, Austria, 2013).

18 Rothen-Rutishauser, B., Riesen, F. K., Braun, A., Gunthert, M. & Wunderli-Allenspach, H. Dynamics of tight and adherens junctions under EGTA treatment. *J Membr Biol* **188**, 151-162; (2002).

19 Glodny, B. *et al.* Normal kidney size and its influencing factors - a 64-slice MDCT study of 1.040 asymptomatic patients. *BMC Urol* **9**, 19; (2009).

20 Harmse, W. S. Normal variance in renal size in relation to body habitus. *SA JOURNAL OF RADIOLOGY*; (2011).

21 van Onna, M. *et al.* Asymmetry of renal blood flow in patients with moderate to severe hypertension. *Hypertension* **41**, 108-113; (2003).

22 Manning, D. K. *et al.* Loss of the ciliary kinase Nek8 causes left-right asymmetry defects. *J Am Soc Nephrol* **24**, 100-112; (2013).

23 Mochizuki, T. *et al.* Cloning of inv, a gene that controls left/right asymmetry and kidney development. *Nature* **395**, 177-181; (1998).

24 Murcia, N. S. *et al.* The Oak Ridge Polycystic Kidney (orpk) disease gene is required for left-right axis determination. *Development* **127**, 2347-2355; (2000).

25 Desai, R. A., Gao, L., Raghavan, S., Liu, W. F. & Chen, C. S. Cell polarity triggered by cell-cell adhesion via E-cadherin. *J Cell Sci* **122**, 905-911; (2009).

26 L. Petitjean, M. R., E. Grasland-Mongrain, M. Poujade, B. Ladoux, A. Buguin, and P. Silberzan. Velocity Fields in a Collectively Migrating Epithelium. *Biophysical Journal* **98**, 1790-1800; (2010).

27 Vedula, S. R. *et al.* Emerging modes of collective cell migration induced by geometrical constraints. *Proc Natl Acad Sci U S A* **109**, 12974-12979; (2012).

28 Marel, A. K. *et al.* Flow and diffusion in channel-guided cell migration. *Biophys J* **107**, 1054-1064; (2014).

29 Vasioukhin, V., Bauer, C., Yin, M. & Fuchs, E. Directed actin polymerization is the driving force for epithelial cell-cell adhesion. *Cell* **100**, 209-219; (2000).

30 Yamada, S., Pokutta, S., Drees, F., Weis, W. I. & Nelson, W. J. Deconstructing the cadherin-catenin-actin complex. *Cell* **123**, 889-901; (2005).

31 Li, L. *et al.* E-cadherin plays an essential role in collective directional migration of large epithelial sheets. *Cell Mol Life Sci* **69**, 2779-2789; (2012).

32 Maruthamuthu, V., Aratyn-Schaus, Y. & Gardel, M. L. Conserved F-actin dynamics and force transmission at cell adhesions. *Curr Opin Cell Biol* **22**, 583-588; (2010).

33 Angelini, T. E. *et al.* Glass-like dynamics of collective cell migration. *Proc Natl Acad Sci U S A* **108**, 4714-4719; (2011).

34 Angelini, T. E., Hannezo, E., Trepat, X., Fredberg, J. J. & Weitz, D. A. Cell migration driven by cooperative substrate deformation patterns. *Phys Rev Lett* **104**, 168104; (2010).

35 Deforet, M., Hakim, V., Yevick, H. G., Duclos, G. & Silberzan, P. Emergence of collective modes and tri-dimensional structures from epithelial confinement. *Nat Commun* **5**, 3747; (2014).

36 Doxzen, K. *et al.* Guidance of collective cell migration by substrate geometry. *Integr Biol (Camb)* **5**, 1026-1035; (2013).

37 Poujade, M. *et al.* Collective migration of an epithelial monolayer in response to a model wound. *Proc Natl Acad Sci U S A* **104**, 15988-15993; (2007).

38 Eisenhoffer, G. T. *et al.* Crowding induces live cell extrusion to maintain homeostatic cell numbers in epithelia. *Nature* **484**, 546-549; (2012).

39 Gros, J., Feistel, K., Viebahn, C., Blum, M. & Tabin, C. J. Cell Movements at Hensen's Node Establish Left/Right Asymmetric Gene Expression in the Chick. *Science* **324**, 941-944; (2009).

40 Lenhart, K. F., Holtzman, N. G., Williams, J. R. & Burdine, R. D. Integration of nodal and BMP signals in the heart requires FoxH1 to create left-right differences in cell migration rates that direct cardiac asymmetry. *PLoS genetics* **9**, e1003109; (2013).

Figures:

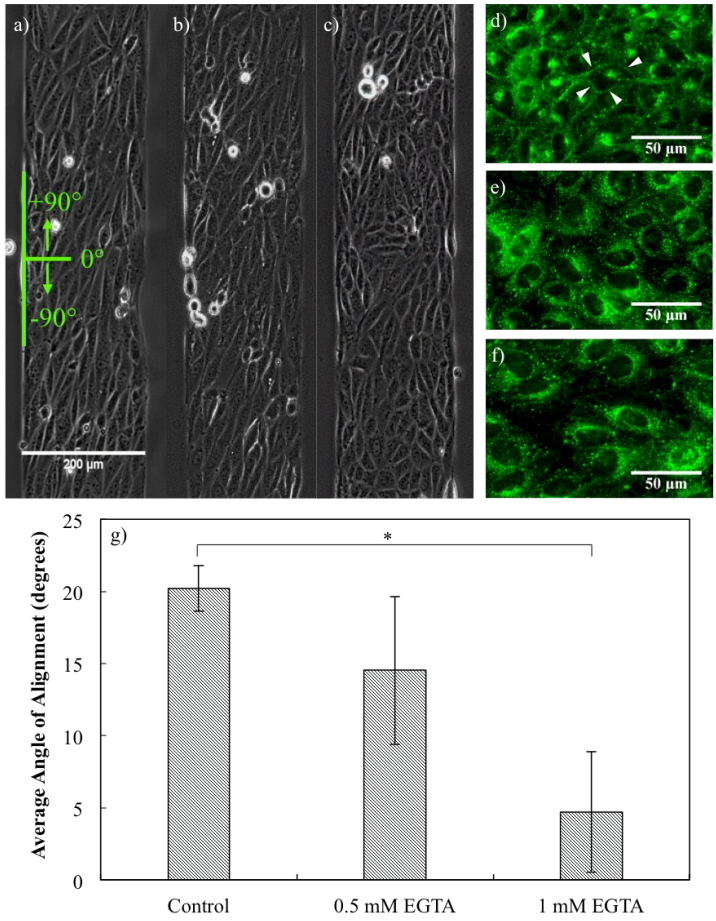

Figure 1. The chiral alignment of MDCK cells is lost with a high EGTA concentration. a-c) Phase contrast images of MDCK cells on 200 µm -width microcontact printed lines for a) untreated; N = 7, b) 0.5 mM EGTA treatment; N = 3, and c) 1.0 mM EGTA treatment; N = 4. d-e) E-cadherin is localized to cell-cell boundaries in d) the control, indicated by the white arrows. It is internalized and cell size increases with the EGTA concentration increase from d) 0 to e) 0.5 mM EGTA and to f) 1.0 mM EGTA. g) The average biased angle of alignment on 200 µm lines decreases with increasing EGTA concentration. The biased angle was determined by examining the cell alignment in relation to the left boundary of the line pattern. The angle is between -90°and +90° with 0° being perpendicular to the boundary. * $p < 0.05$.

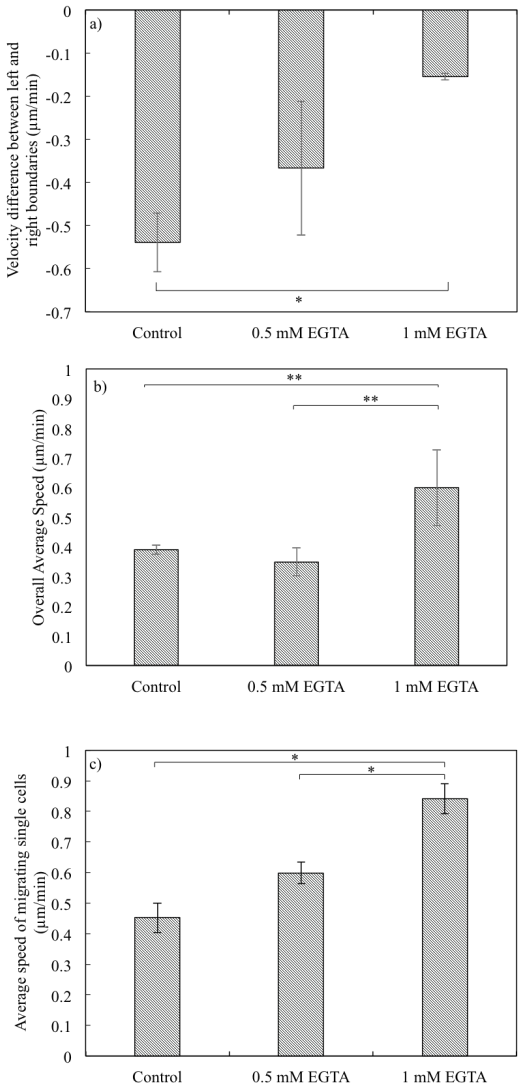

Figure 2. Treatment with EGTA increases cell motility in confluent and single cells, but decreases directionality. a) Velocity difference between the left and right boundaries on 200 µm lines decreases with the increase of EGTA concentration. The negative value indicates that cells on the left boundary migrate downwards while those on the right migrate upwards. b) The overall average speed increases with increasing EGTA concentration. A decrease in adherens junctions leads to an increase in migration speed. c) Treatment of sparsely seeded MDCK cells with EGTA shows an increase in migration speed with increasing EGTA concentration (Control: N = 49; 0.5 mM EGTA: N = 23; 1 mM EGTA: N = 23). * $p < 0.1$; ** $p < 0.05$.

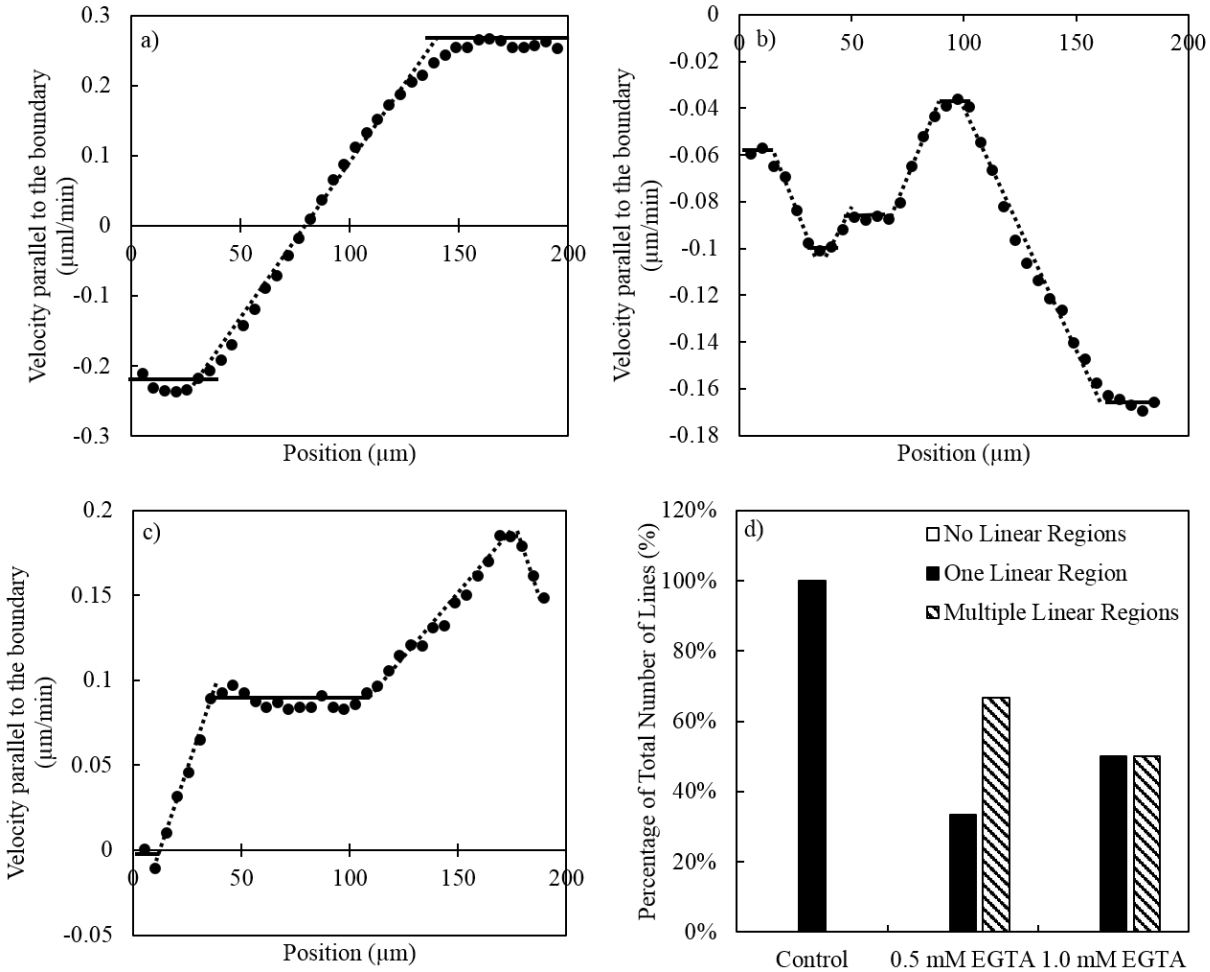

Figure 3. A decrease in adherens junction formation results in greater variability in velocity profile across the line width. a) An untreated 200 μm line exhibiting a single linear slope. The solid lines accent the plateau regions on each boundary and the connecting linear region as denoted by dotted lines. b) A 200 μm line treated with 0.5 mM EGTA exhibiting a variable slope. c) A 200 μm line treated with 1.0 mM EGTA exhibiting a variable slope. d) Untreated 200 μm lines consistently exhibit one linear region. The EGTA treated groups show more variability in the number of linear regions.

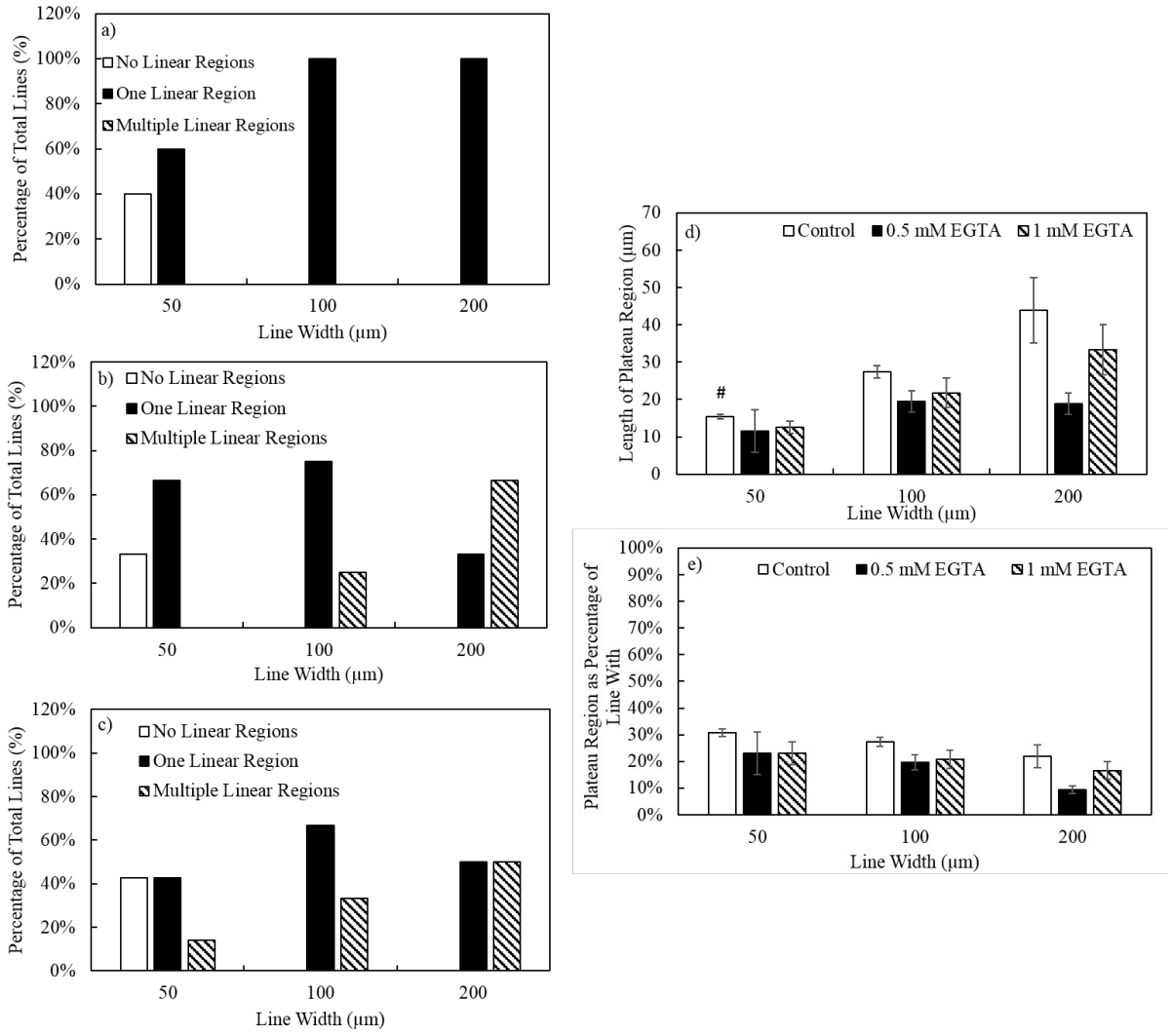

Figure 4. Decreasing the width of the patterned line causes a decrease in the plateau region and decrease in the variability of the velocity across the line width. a) Untreated cells on patterned lines exhibit linear changes in velocity across the width except for the 50 μm line, where some exhibit no change in velocity across the width (200 μm: N = 7; 100 μm: N = 5; 50 μm: N = 5). b) MDCK cells treated with 0.5 mM EGTA on patterned lines (200 μm: N = 3; 100 μm: N = 4; 50 μm: N = 3). c) MDCK cells treated with 1.0 mM EGTA on patterned lines (200 μm: N = 4; 100 μm: N = 6; 50 μm: N = 7). d) Decreasing line width decreases the length of the plateau region and negates the difference in plateau region due to treatment with EGTA. # $p < 0.05$ when

compared to the 200 μm group at the same EGTA concentration. e) The plateau region of control lines is slightly larger as a proportion of total line width than for EGTA treated lines.

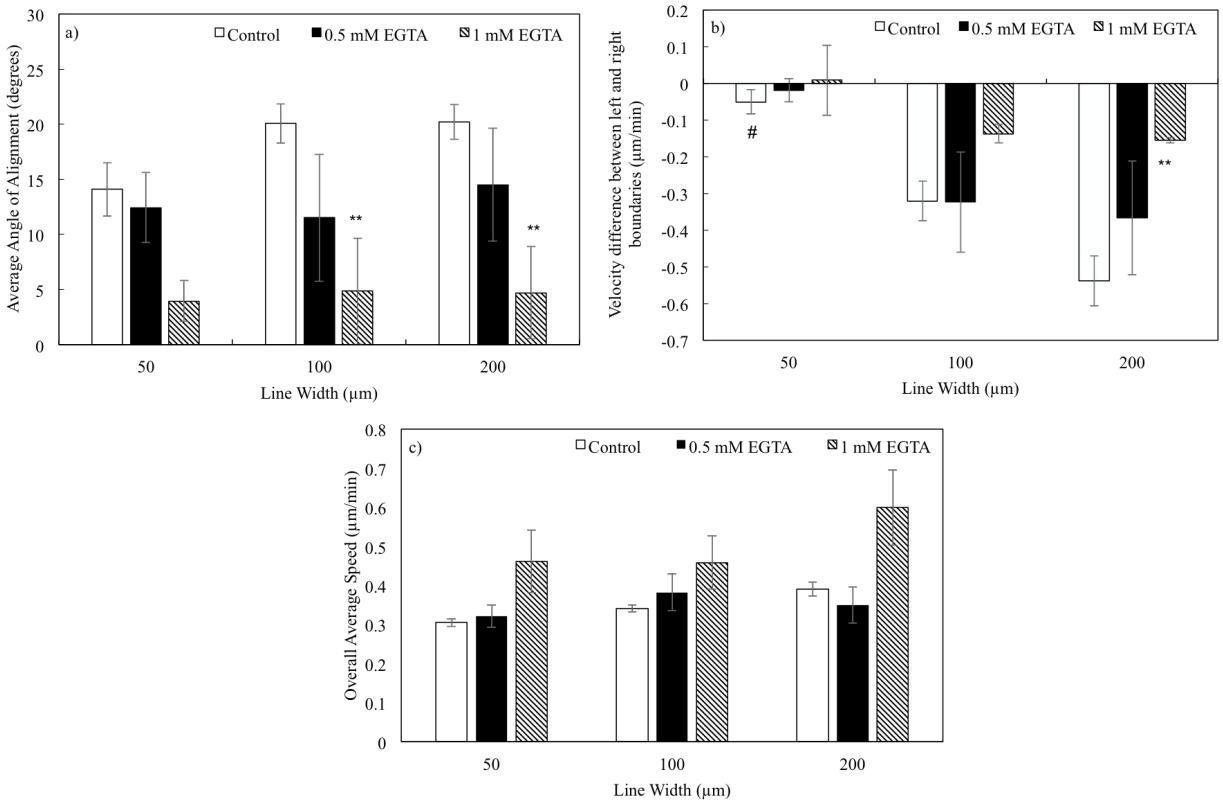

Figure 5. Decreasing the width of the patterned line causes a decrease in alignment and a decrease in the magnitude of the difference in velocity between the boundaries, but does not influence speed. a) The angle of alignment decreases for 50 μm control lines b) Decreasing line width decreases the magnitude of the velocity difference between boundaries, but no difference is indicated for the 50 μm line. c) Overall average speed does not change with line width. # $p < 0.05$ when compared to the 200 μm group at the same EGTA concentration, and ** $p < 0.1$ when compared to the control group with the same width.

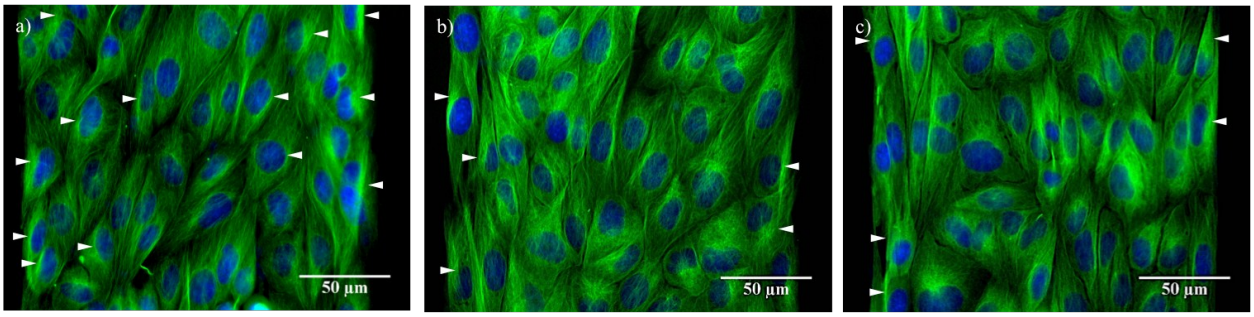

Figure 6. Internal polarization of the cells is consistent at the boundaries regardless of treatment but disruption of adherens junctions decreases transmission of chiral bias to the adjacent interior cells. a-c) The centrosome, visible by the bright green area and accented by the white arrows, is positioned toward the boundary in comparison to the nucleus (blue) for border cells regardless of treatment: a) untreated control, b) 0.5 mM EGTA, and c) 1.0 mM EGTA. However, boundary dependent internal polarization is only seen for interior cells of the control (a).

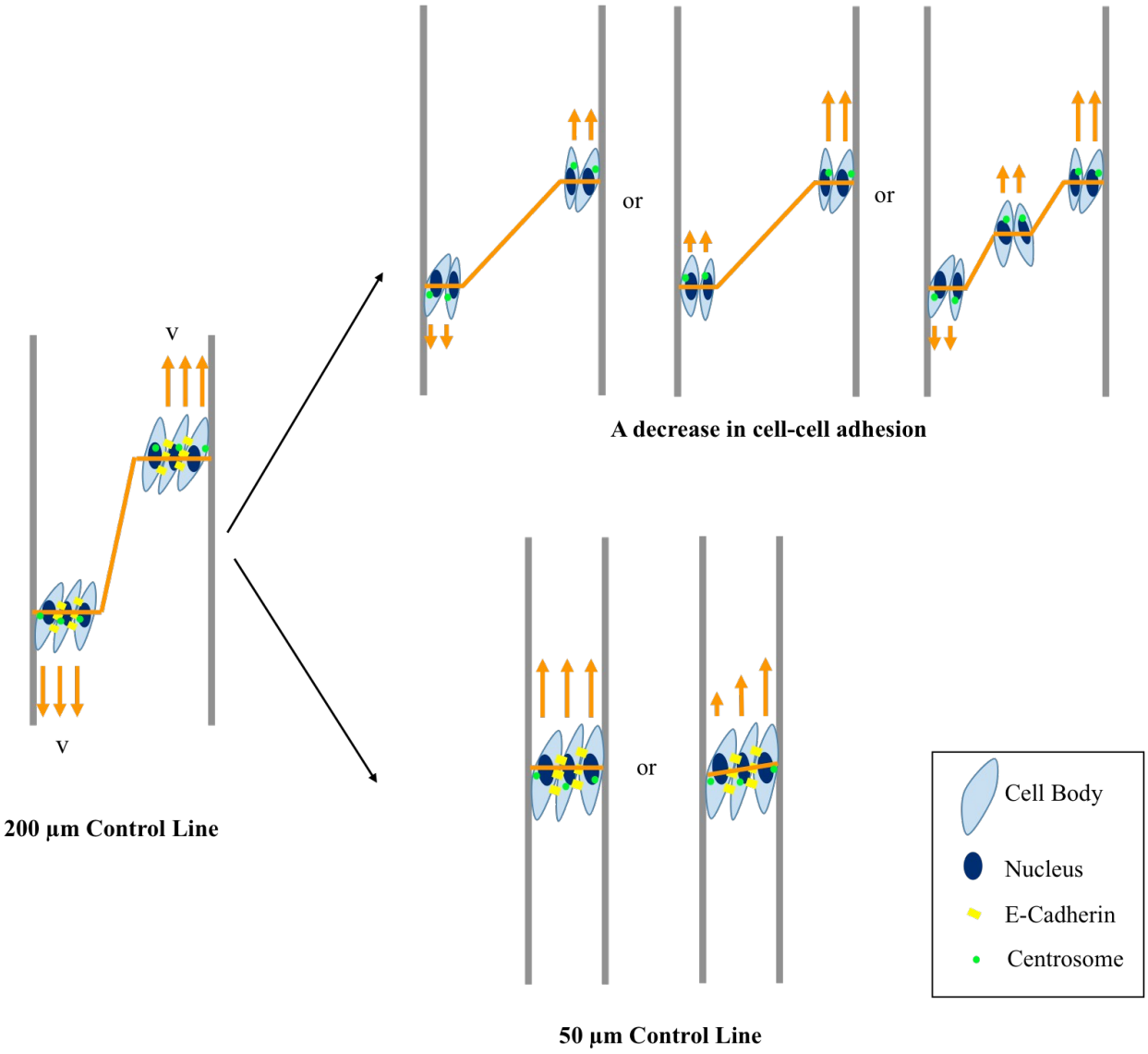

Figure 7. A diagram of how decreasing cell-cell adhesion and line width causes alterations in the ability of cells to migrate collectively and transfer boundary information. Decreasing cell-cell adhesion causes the cells to migrate more randomly resulting in a variety of potential migration outcomes. Decreasing line width often causes confounding boundary information with the end result being overall migration in the same direction.